Int. J. Heat Mass Transfer. Vol. 15, pp. 2241–2250. Pergamon Press 1972. Printed in Great Britain

THE EFFECTS OF LIQUID MOTION INDUCED BY PHASE CHANGE AND THERMOCAPILLARITY ON THE THERMAL EQUILIBRIUM OF A VAPOUR BUBBLE

E. S. GADDIS

Atomic Energy Establishment of A.R.E., Reactor Department, Inchass, Cairo, Egypt

(*Received* 29 *June* 1970 *and in revised form* 29 *September* 1971)

Abstract—A theoretical estimate is made of the liquid motion induced in the vicinity of a vapour bubble on a heated solid surface by evaporation and condensation at the bubble surface and by thermocapillarity effects. These results are used to examine the thermal equilibrium of the vapour bubble.

It is found that whilst the effects of convection induced by evaporation and condensation are small, the effects of thermocapillarity may be important in determining the temperature of the equilibrium bubble.

NOMENCLATURE

a, bubble radius;

c, liquid specific heat

E^2, $\dfrac{\partial^2}{\partial r^{*2}} + \dfrac{\sin\theta}{r^{*2}}\dfrac{\partial}{\partial\theta}\left(\dfrac{1}{\sin\theta}\dfrac{\partial}{\partial\theta}\right)$;

F, $\dfrac{\zeta^*}{r^*\sin\theta}$;

G, $r^*\sin\theta\zeta^*$;

h, heat transfer coefficient at liquid–vapour interface;

k, liquid thermal conductivity;

L, latent heat of evaporation;

M, molecular weight;

M_k, Marangoni number $\left[= \dfrac{q_{w\infty}a^2c\rho}{k^2\mu}\left(-\dfrac{\partial\delta}{\partial T}\right)\right]$;

N, dimensionless quantity associated with the evaporation and condensation at the bubble surface $\left[= \dfrac{q_{w\infty}a^2ch}{k^2L}\right]$,

Pr, liquid Prandtl number;

p, pressure;

p_v, saturated vapour pressure corresponding to temperature T_v;

Q, heat flow through bubble surface;

q_w, wall heat flux;

$q_{w\infty}$ undisturbed wall heat flux;

R, universal gas constant;

r, radial distance;

r_f, radius of sphere containing bubble disturbance;

T, temperature;

T_a, liquid undisturbed temperature at a distance from the wall equal to bubble radius;

T_v, vapour temperature;

$T_{w\infty}$, undisturbed wall surface temperature;

u, radial velocity;

v, tangential velocity;

y_m, distance in liquid where the undisturbed liquid and vapour have identical temperatures;

Z, $\ln r^*$;

Z_f, $\ln r_f^*$;

α, bubble Nusselt number $[= ha/k]$;

ΔZ, mesh size in radial direction;

$\Delta\theta$, mesh size in tangential direction;

ζ, vorticity;

θ, angle measured from bubble axis;

μ, liquid dynamic viscosity;

ρ, liquid density;

σ, surface tension;

τ, shear stress;

Ψ, stream function.

* asterisked symbols are dimensionless and defined in the paper.

1. INTRODUCTION

CURRENT theories predicting the commencement of nucleate boiling at a heated solid surface in contact with a liquid, depend on a model for the thermal equilibrium of a bubble nucleus in a region in which the liquid temperature changes rapidly with distance from the heated surface (Han and Griffith [1], Hsu [2], Bergles and Rohsenow [3], Sato and Matsumura [4], Davis and Anderson [5] and Kenning and Cooper [6]).

Theoretical models describing the thermal equilibrium of a vapour bubble differ in the emphasis placed on the mechanism by which heat flow to the bubble. Thus, Kenning and Cooper [6] studied the case when the heat flow to the vapour bubble is solely by convection in the thermal layer induced by a forced flow. In this limiting case the bubble temperature assumes the temperature of the stagnation stream line. Gaddis and Hall [7] have presented a model of a vapour bubble in thermal equilibrium on a heated solid surface when the mechanism of heat transfer in the liquid is by conduction but when evaporation occurs over part of the bubble surface and condensation over the rest. The analysis has shown that there are temperature variations between local points on the bubble surface and the vapour temperature inside the bubble which may be significant especially near the bubble base. These temperature variations create two factors which may induce convection in the liquid surrounding the bubble. The first arises from evaporation and condensation at the bubble surface near its base and tip respectively, and the second from variations of surface tension due to variations of temperature over this interface.

The work presented in this paper is complementary to that in [7], its purpose is to study the motion that is induced in the vicinity of the bubble by the above factors, and to investigate its effect on the thermal equilibrium of the vapour bubble. The analysis is based on a simultaneous numerical solution of the equations of motion and the energy equation.

2. DESCRIPTION OF THE MODEL

The model is illustrated in Fig. 1, where a vapour bubble sits on a cavity in a state of

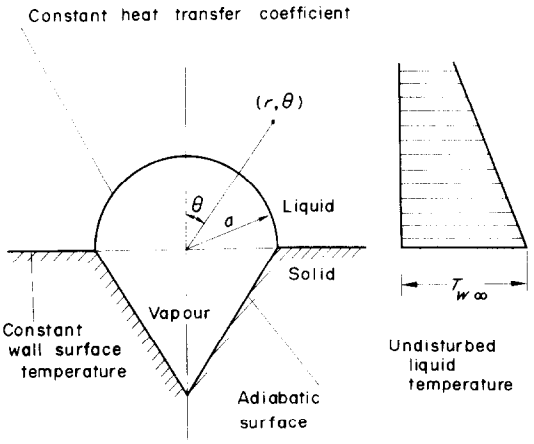

FIG. 1. Illustration of thermal boundary conditions.

thermal equilibrium. The following assumptions are made:

1. Physical properties are constant.
2. Wall surface temperature is constant.
3. Vapour pressure and temperature inside the bubble are uniform.
4. Fluid is pure.
5. The mechanism of evaporation or condensation at an interface between a pure liquid and its vapour is usually viewed from the standpoint of the kinetic theory of gases as a difference between two quantities—a rate of departure of molecules from the surface of the liquid into the vapour space and a rate of arrival of molecules from the vapour space toward the interface. When evaporation takes place the departure rate exceeds the arrival rate and vice-versa, during equilibrium the two rates are equal. An expression of the heat transfer coefficient associated with the mass transfer of the fluid through the liquid vapour interface has been derived in [7]. It has been assumed that the evaporation and condensation coefficients for a pure fluid are equal to unity and that the vapour molecules have

velocity distribution identical with the Maxwellian distribution. The heat transfer coefficient at the liquid–vapour interface derived under these assumptions, is given by,

$$h = L\left(\frac{M}{2\pi RT_v}\right)^{\frac{1}{2}}\left[\left(\frac{\mathrm{d}p}{\mathrm{d}T}\right)_{T_v} - \frac{1}{2}\left(\frac{p_v}{T_v}\right)\right] \quad (1)$$

and is uniform at the whole surface of the bubble nucleus.

6. The vapour bubble has a hemispherical shape.
7. The bubble radius is considerably smaller than the thickness of the non-turbulent layer near the solid boundary.
8. The fluid is assumed initially to be stationary and with linear temperature gradient.
9. No interaction occurs between neighbouring bubbles.
10. Direct heat flow from solid to vapour through solid–vapour interface is ignored.

3. FORMULATION OF THE PROBLEM

3.1 *Equations of motion*

The equations of motion are treated as in (8). In dimensionless form the equations may be presented as

$$E^2\Psi^* + G = 0 \quad (2)$$

$$E^2G + \frac{\sin\theta}{Pr}\left[\frac{\partial\Psi^*}{\partial r^*}\frac{\partial F}{\partial\theta} - \frac{\partial\Psi^*}{\partial\theta}\frac{\partial F}{\partial r^*}\right] = 0 \quad (3)$$

where

$$G = r^*\sin\theta\zeta^*$$

$$F = \frac{\zeta^*}{r^*\sin\theta}$$

$$E^2 = \frac{\partial^2}{\partial r^{*2}} + \frac{\sin\theta}{r^{*2}}\frac{\partial}{\partial\theta}\left(\frac{1}{\sin\theta}\frac{\partial}{\partial\theta}\right).$$

The dimensionless velocity components are related to the dimensionless stream function as

$$u^* = \frac{1}{r^{*2}\sin\theta}\frac{\partial\Psi^*}{\partial\theta} \quad (4)$$

$$v^* = -\frac{1}{r^*\sin\theta}\frac{\partial\Psi^*}{\partial r^*} \quad (5)$$

and the dimensionless quantities are defined by

$$r^* = \frac{r}{a} \quad = \text{dimensionless radial distance}$$

$$u^* = \frac{a\rho cu}{k} \quad = \text{dimensionless radial velocity}$$

$$v^* = \frac{a\rho cv}{k} \quad = \text{dimensionless tangential velocity}$$

$$\Psi^* = \frac{\rho c\Psi}{ka} \quad = \text{dimensionless stream function}$$

$$\zeta^* = \frac{a^2\rho c\zeta}{k} = \text{dimensionless vorticity.}$$

If the inertia effects are small compared to viscous effects, the inertia term in equation (3) can be eliminated and the equation becomes

$$E^2G = 0. \quad (6)$$

3.2 *Energy equation*

The energy equation may be presented in a dimensionless form as

$$\frac{\partial^2T^*}{\partial r^{*2}} + \frac{2}{r^*}\frac{\partial T^*}{\partial r^*} + \frac{1}{r^{*2}}\frac{\partial^2T^*}{\partial\theta^2} + \frac{\cot\theta}{r^{*2}}\frac{\partial T^*}{\partial\theta} = \frac{1}{r^{*2}\sin\theta}\left(\frac{\partial T^*}{\partial r^*}\frac{\partial\Psi^*}{\partial\theta} - \frac{\partial T^*}{\partial\theta}\frac{\partial\Psi^*}{\partial r^*}\right). \quad (7)$$

The dimensionless temperature is defined by

$$T^* = \frac{T - T_{w\infty}}{T_a - T_{w\infty}} = -\frac{(T - T_{w\infty})k}{aq_{w\infty}}.$$

3.3 *Boundary conditions*

The temperature, the stream function and the vorticity fields must be specified at all points around a closed boundary.

3.3.1 *Far from the bubble.* The disturbances caused by the bubble in both the temperature and velocity fields decay as the distance from the bubble centre is increased. A hemisphere is imagined of an arbitrary radius r_f^*, which is concentric with the hemispherical bubble. If the radius of the hemisphere is chosen big enough, the liquid outside this hemisphere will not be affected by the presence of the bubble. Thus,

the temperature distribution at this hemispherical surface is fixed from the original linear temperature distribution, and the stream function and vorticity are zero. The choice of the radius r_f^* must be such that increasing it further bears no effect on both the temperature and velocity fields in the vicinity of the bubble.

Thus, at $r^* = r_f^*$ the following relations must be fulfilled:

$$(T^*)_{r^*=r_f^*} = r_f^* \cos\theta \tag{8}$$

$$(\Psi^*)_{r^*=r_f^*} = 0 \tag{9}$$

$$(G)_{r^*=r_f^*} = 0. \tag{10}$$

3.3.2 *At the axis of symmetry.* From symmetry

$$\left(\frac{\partial T^*}{\partial \theta}\right)_{\theta=0} = 0 \tag{11}$$

$$(\Psi^*)_{\theta=0} = 0 \tag{12}$$

$$(G)_{\theta=0} = 0. \tag{13}$$

3.3.3 *At the liquid–vapour interface.* The thermal boundary condition at the bubble surface is

$$k\left(\frac{\partial T}{\partial r}\right)_{r=a} = h[(T)_{r=a} - T_v].$$

The previous equation may be expressed in a dimensionless form as

$$\left(\frac{\partial T^*}{\partial r^*}\right)_{r^*=1} = \alpha[(T^*)_{r^*=1} - T_v^*] \tag{14}$$

where

$$\alpha = \frac{ha}{k} \text{ (bubble Nusselt number).}$$

The radial velocity at the bubble surface is related to the surface temperature by

$$\rho L(u)_{r=a} = h[T_v - (T)_{r=a}].$$

The previous equation may be presented in a dimensionless form as

$$(u^*)_{r^*=1} = N[(T^*)_{r^*=1} - T_v^*] \tag{15}$$

where

$$N = \frac{q_{w\infty} a^2 ch}{k^2 L}.$$

The dimensionless parameter N is the product of the bubble Nusselt number and the dimensionless quantity $(q_{w\infty} ac/kL)$.

The relation between the radial velocity and the stream function at the bubble surface is obtained from equation (4), or

$$(\Psi^*)_{r^*=1} = \int_0^\theta (u^*)_{r^*=1} \sin\theta \, d\theta$$

substituting from equation (15) gives

$$(\Psi^*)_{r^*=1} = N\left[\int_0^\theta (T^*)_{r^*=1} \sin\theta \, d\theta - (1 - \cos\theta) T_v^*\right]. \tag{16}$$

At the bubble base

$$(\Psi^*)_{r^*=1,\,\theta=\pi/2} = N\left[\int_0^{\pi/2} (T^*)_{r^*=1} \sin\theta \, d\theta - T_v^*\right]$$

and from the condition of thermal equilibrium (see equation (29)), the stream function at the bubble base becomes

$$(\Psi^*)_{r^*=1,\,\theta=\pi/2} = 0. \tag{17}$$

To fix the vorticity at the bubble surface a second relation is required between the stream function and the temperature. This is obtained from the dependance of the shear stress at the liquid–vapour interface on the temperature gradient. From the balance of forces acting on an infinitesimal ring on the bubble surface, it can be shown that

$$(\tau)_{r=a} = \frac{1}{a}\frac{\partial \delta}{\partial \theta} = \frac{1}{a}\left(\frac{\partial \delta}{\partial T}\right)\left(\frac{\partial T}{\partial \theta}\right)_{r=a}.$$

The previous expression may be presented in a dimensionless form as

$$(\tau^*)_{r^*=1} = M_k\left(\frac{\partial T^*}{\partial \theta}\right)_{r^*=1} \tag{18}$$

where

$$\tau^* = \frac{a^2 \rho c \tau}{\mu k}$$

and

$$M_k = \frac{q_{w\infty} a^2 c \rho}{k^2 \mu}\left(-\frac{\partial \delta}{\partial T}\right) \text{(Marangoni number)}.$$

It is of interest to notice that the Marangoni number M_k is the product of the dimensionless parameter N and the dimensionless quantity $[(\rho L/h\mu)(-\partial\delta/\partial T)]$. The latter quantity is a function only of the physical properties of the fluid and does not depend on the wall heat flux or the bubble radius. Thus for any particular fluid, M_k varies linearly with N as N varies with the wall heat flux or the bubble size.

The shear stress in the liquid can be related to the stream function [9]. At the bubble surface, the shear stress applied on the liquid from the interface may be expressed in a dimensionless form as

$$(\tau^*)_{r^*=1} = \frac{1}{\sin\theta}\left[\frac{\partial^2 \Psi^*}{\partial r^{*2}} - 2\frac{\partial \Psi^*}{\partial r^*} - \frac{\partial^2 \Psi^*}{\partial \theta^2} + \cot\theta \frac{\partial \Psi^2}{\partial \theta}\right]_{r^*=1}. \quad (19)$$

Equating the two shear stress expressions gives

$$\left[\frac{\partial^2 \Psi^*}{\partial r^{*2}} - 2\frac{\partial \Psi^*}{\partial r^*} - \frac{\partial^2 \Psi^*}{\partial \theta^2} + \cot\theta \frac{\partial \Psi^*}{\partial \theta}\right]_{r^*=1} = M_k \sin\theta \left(\frac{\partial T^*}{\partial \theta}\right)_{r^*=1}. \quad (20)$$

3.3.4 *At the liquid–solid interface.* The thermal boundary condition at the liquid–solid interface is

$$(T^*)_{\theta=\pi/2} = 0. \quad (21)$$

The hydrodynamic boundary conditions at the liquid–solid interface are

$$(u^*)_{\theta=\pi/2} = 0 \quad (22)$$

$$(v^*)_{\theta=\pi/2} = 0 \quad (23)$$

hence from equations (4) and (5)

$$\left(\frac{\partial \Psi^*}{\partial \theta}\right)_{\theta=\pi/2} = 0 \quad (24)$$

$$\left(\frac{\partial \Psi^*}{\partial r^*}\right)_{\theta=\pi/2} = 0. \quad (25)$$

Equations (22)–(25) are valid at $r^* > 1$. At the bubble base there is a discontinuous change in the velocity components created by the contradicting requirements of the thermal and hydrodynamic boundary conditions.

From equation (25)

$$(\Psi^*)_{\theta=\pi/2} = \text{constant}$$

but since

$$(\Psi^*)_{\theta=\pi/2} = 0 \quad \text{at} \quad r^* = 1 \quad \text{and at} \quad r^* = r_f^*$$

hence

$$(\Psi^*)_{\theta=\pi/2} = 0 \quad \text{at} \quad 1 \leqslant r^* \leqslant r_f^* \quad (26)$$

also

$$\left(\frac{\partial^2 \Psi^*}{\partial r^{*2}}\right)_{\theta=\pi/2} = 0 \quad \text{at} \quad 1 < r^* \leqslant r_f^*. \quad (27)$$

Substituting in equation (2) gives

$$(G)_{\theta=\pi/2} = -\frac{1}{r^{*2}}\left(\frac{\partial^2 \Psi^*}{\partial \theta^2}\right)_{\theta=\pi/2} \quad \text{at} \quad 1 < r^* \leqslant r_f^*. \quad (28)$$

3.4 *Condition for thermal equilibrium*

Equilibrium is attained when there is a balance between evaporation and condensation i.e. when there is no net heat flow to the vapour bubble, or

$$Q = 2\pi a^2 h \int_0^{\pi/2} [T_v - (T)_{r=a}] \sin\theta \, d\theta = 0.$$

Thus, the condition for thermal equilibrium may be expressed in a dimensionless form as

$$T_v^* = \int_0^{\pi/2} (T^*)_{r^*=1} \sin\theta \, d\theta. \quad (29)$$

In many cases the results are summarized

by quoting the value of the dimensionless distance y_m^*, where

$$y_m^* = \frac{y_m}{a}$$

and y_m is the distance in the liquid from the liquid–solid interface where the undisturbed liquid and the vapour in the equilibrium bubble have identical temperatures. It is clear that

$$y_m^* = T_v^*.$$

From equations (3), (14), (15) and (20), it appears that the mathematical solution should be described by the dimensionless quantities Pr, α, N and M_k. Typical values for pure water boiling at atmospheric pressure ($h = 7{\cdot}7 \times 10^3$ kW/m^2°C) with wall heat flux 200 kW/m^2 are as follows: if the bubble radius is 1 μm, then $\alpha \approx 10$, $N \approx 0{\cdot}005$ and $M_k \approx 1{\cdot}25$, and if the bubble radius is 10 μm, then $\alpha \approx 100$, $N \approx 0{\cdot}5$ and $M_k \approx 125$.

4. NUMERICAL RESULTS

The lattice is constructed as in [8]. The transformation $r^* = \exp(Z)$ is made and equal intervals in Z are used. This leads to a small mesh size near the bubble surface (where stream function and vorticity change most rapidly) and a coarser mesh size at a distance from the bubble.

The radius of the outer sphere r_f^* is taken in the computation as $r_f^* = \exp(2) = 7{\cdot}39$ or $Z_f = 2$. Few calculations were repeated for higher values of r_f^*, the corresponding change in the temperature field near the bubble surface was insignificant. For example, when $\alpha = 10$, $N = 0{\cdot}05$ and $M_k = 125$ the change in y_m^* was not more than 3 per cent when r_f^* was increased from 7·39 ($Z_f = 2$) to 54·6 ($Z_f = 4$).

The radial step ΔZ and the angular step $\Delta\theta$ were chosen such that computational errors were kept small. To examine the accuracy associated with the chosen mesh size, the computed results obtained from this numerical analysis in the case when conduction is the only mechanism of heat transfer in the liquid ($N = 0$, $M_k = 0$) were compared with the corresponding results obtained from the series solution described in [7] for the case of a highly conducting wall (constant wall surface temperature). The comparison is shown in Table 1.

Table 1. Comparison of series and numerical solutions for the case of a highly conducting wall (constant wall surface temperature), and no flow ($N = 0$, $M_k = 0$)

	y_m^*		Mesh parameters	
α	Series solution (from [7])	Numerical solution (present calculation)	ΔZ	$\Delta\theta$ (approximate)
0	0·75	0·75	0·050	0·050
1	0·70	0·69	0·050	0·050
10	0·54	0·52	0·050	0·050
100	0·37	0·34	0·025	0·025

Few cases were considered to investigate the inertia effects on y_m^*. For example computation was made for the case when $\alpha = 10$, $N = 0{\cdot}05$, $M_k = 125$ and $Pr = 2$. This nearly represents the case of water at atmospheric pressure with a wall heat flux of 200 kW/m^2 when the radius of the equilibrium bubble is 10 μm. The heat transfer coefficient at the liquid–vapour interface was taken as 770 kW/m^2°C, or 0·1 of the theoretical value given by equation (1), the reduced value may be regarded due to the presence of contaminants or non-condensable gases in the fluid. The computation was repeated ignoring the inertia term in equation (3). The computed values of y_m^*, were the same, also temperature variations at the bubble surface between the two cases were insignificant. The same procedure was repeated with $\alpha = 1$, $N = 0{\cdot}005$, $M_k = 1{\cdot}25$ and $Pr = 0{\cdot}1$. The parameters were chosen in this case nearer to the liquid metal case (for the same wall heat flux and bubble size, liquid metals have much lower values of α, N and M_k than water). Also, no change was found in y_m^* when the inertia term was eliminated from the equation of motion. In the rest of the computations, equation (6) was considered instead of equation (3).

To investigate the effects of liquid motion

induced by the evaporation and condensation of the fluid at the liquid–vapour interface on y_m^*, computations were made at different values of α and N for the particular case when $M_k = 0$. The computed values of y_m^* are shown in Table 2. The parameter N was given increasing values in Table 2 as α was increased, since N is the product of α and the dimensionless quantity $(q_{w\infty}ac/kL)$. Thus, α has a direct effect on N, and in the limiting case when $\alpha = 0$ the parameter N equals zero for all finite values of the quantity $(q_{w\infty}ac/kL)$. When M_k has a zero value the shear stress at the bubble surface vanishes (see equation (18)), and thermocapillary flow stops. In this case, the liquid motion in the vicinity of the bubble is induced only by evaporation and condensation. Thus, the particular cases when $N = 0$ in Table 2 correspond to the purely conduction problem. Increasing N induces liquid flow by evaporation and condensation at the interface, which might affect y_m^* through the non-linearity in equation (7). However, Table 2 shows no such effect, hence the non-linearity has little effect on y_m^* in the cases studied here. Hence, in these cases, the flow due to evaporation and condensation has little effect on y_m^* in the absence of thermocapillarity. Similar behaviour was also observed when thermocapillary flow was present (M_k has non-zero value).

Table 2. Computed values of y_m^* *at different values of* α *and* N *for the particular case when* $M_k = 0$

N	α			
	0	1	10	100
0	0·75	0·69	0·52	0·34
0·1	—	0·69	↓	↓
1	—	—	0·52	↓
10	—	—	—	0·34

Since the parameter N is irrelevant to the problem in the considered cases, the variations in the computed values of y_m^* are, then, only due to variations in α and M_k. It becomes, then, reasonable to consider that, for this range, y_m^* is only a function of the bubble Nusselt number and the Marangoni number. The computed values of y_m^* at different values of α and M_k are shown in Table 3 and summarized in Fig. 2. From Fig. 2 it appears that at low values of the bubble Nusselt number ($\alpha \leqslant 1$) thermocapillary flow becomes effective in modifying y_m^* even at low values of the Marangoni number as $M_k = 1$. At higher values of the bubble Nusselt number ($\alpha > 1$) thermocapillary flow becomes effective only when the Marangoni number exceeds a

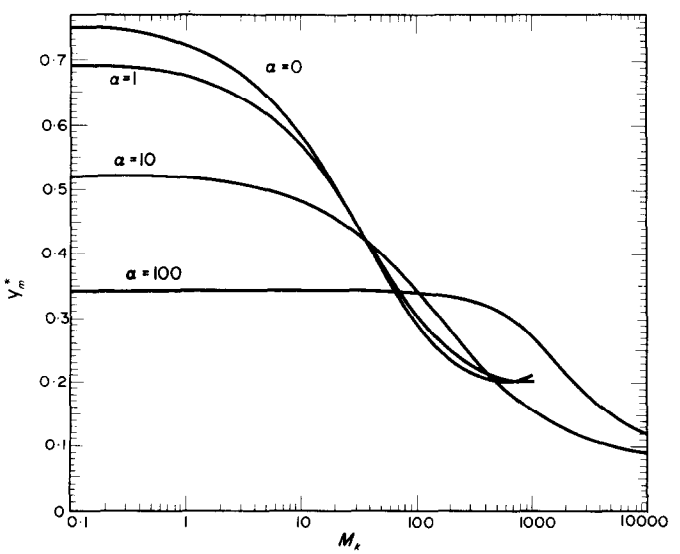

FIG. 2. y_m^* against M_k for different values of α.

Table 3. Computed values of y_m^* as a function of α and M_k

M_k	α			
	0	1	10	100
0	0·75	0·69	0·52	0·34
1	0·73	0·68	0·52	↓
10	0·59	0·58	0·49	
100	0·30	0·31	0·35	0·34
1000	0·21	0·20	0·16	0·28
10000	—	—	0·09	0·12

value of the order of magnitude of the bubble Nusselt number.

Typical distributions of the wall heat flux in the vicinity of the bubble are shown in Fig. 3, and a typical set of stream lines is illustrated in Fig. 4. Further details are given in [10].

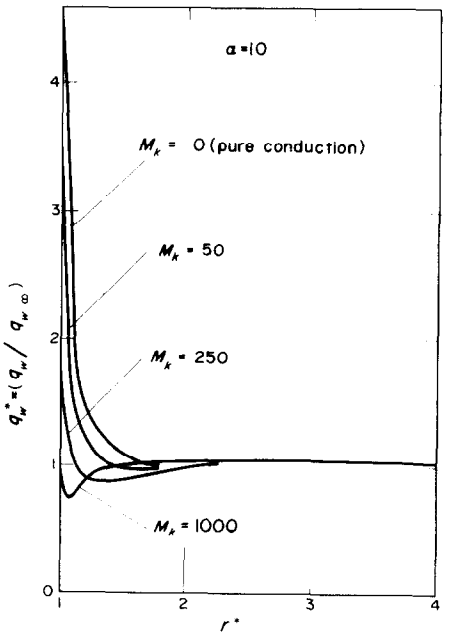

FIG. 3. Wall heat flux against distance from bubble centre.

5. THERMOCAPILLARITY EFFECTS ON y_m^* IN CERTAIN CASES

Using the data given at the end of section (3) with $\alpha = 10$, $M_k = 1{\cdot}25$ for the smaller bubble (1μm) and $\alpha = 100$, $M_k = 125$ for the larger bubble (10μm), it can be seen from Fig. 2 that thermocapillarity would have insignificant effect on y_m^* for either bubble. In each case y_m^* has its

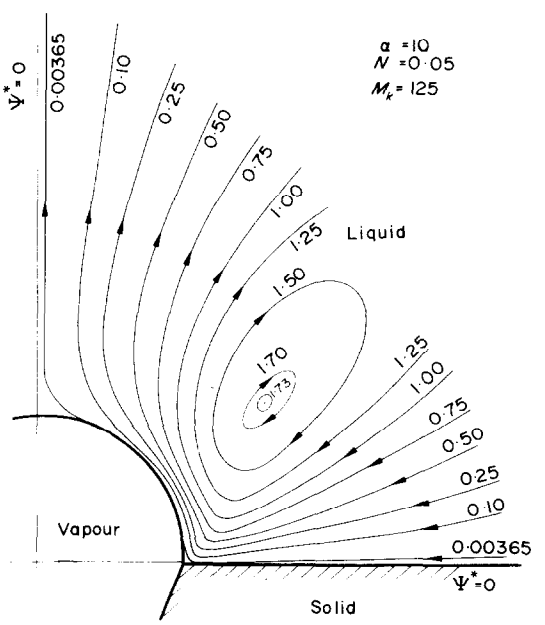

FIG. 4. Stream lines around a vapour bubble.

value for the stationary conduction problem. If it is assumed that h is reduced by a factor of 10 (due to contamination of fluid), then α is reduced by a factor of 10 while M_k is unchanged. Figure 2 then shows that thermocapillarity would hardly affect y_m^* on the smaller bubble, but it would affect y_m^* on the larger bubble reducing it to some 60 per cent of the value for the stationary conduction problem. Proceeding to the limiting case when the bubble surface is adiabatic gives a value of $\alpha = 0$ for both cases (M_k still does not change). In this case thermocapillarity has little effect on the smaller bubble, but its effect on the larger bubble is increased further reducing y_m^* to about 40 per cent of the conduction value.

6. CONCLUSION

The analysis has shown that whilst the effects of convection induced by evaporation and condensation on y_m^* are small in the considered cases, the effects of thermocapillarity may be significant.

An important factor that has a significant role in relation to thermocapillarity is the level of heat transfer coefficient at the liquid–vapour interface. High heat transfer coefficients reduce thermocapillary flow. In fact thermocapillarity has its utmost effect when the bubble surface is adiabatic. However, high heat transfer coefficients increase bubble temperature due to conduction alone.

The numerical results show that thermocapillarity reduces y_m^* compared with the conduction value. Hence, in the range of the computed results, thermocapillary flow reduces the temperature difference between the wall surface and the vapour inside the equilibrium bubble. Thus, including thermocapillarity effects in the conduction model leads to lower wall superheat for nucleation and lower wall surface temperature for the incipience of boiling.

The method of calculation presented in this paper fails to deal with big bubbles penetrating outside the non-turbulent layer. However, thermocapillarity may still be important in these cases. Such bubbles have, in fact, considerable temperature differences over their surfaces, since the temperature at the bubble tip is governed by the liquid bulk temperature, while the temperature at the bubble base is governed by the local wall surface temperature. Thermocapillarity may be further enhanced in such situations, by the presence of foreign substances in the fluid due to restricting evaporation and condensation at the interface, this may cause a redistribution of the temperature difference at the bubble surface.

ACKNOWLEDGEMENT

This research has been made in the period from 1966 to 1968 in the Nuclear Engineering Department—University of Manchester. The author wishes to acknowledge the considerable assistance he has received from Professor W. B. Hall.

REFERENCES

1. C. Y. Han and P. Griffith, The mechanism of heat transfer in nucleate pool boiling, *Int. J. Heat Mass Transfer* **8**, 887–904 (1965).
2. Y. Y. Hsu, On the size range of active nucleation cavities on a heating surface, *J. Heat Transfer* (August 1962).
3. A. E. Bergles and W. M. Rohsenow, The determination of forced convection surface boiling heat transfer, *J. Heat Transfer* (August 1964).
4. T. Sato and H. Matsumura, *Bull. JSME* **7**, 392 (1964).
5. E. J. Davis and G. H. Anderson, The incipience of nucleate boiling in forced convection flow, *A.I.Ch.E. Jl* (July 1966).
6. D. B. R. Kenning and M. G. Cooper, Flow patterns near nuclei and the initiation of boiling during forced convection heat transfer, paper 11, Symp. Boiling Heat Transfer, Proc. Instn mech. Engrs. 180, Pt 3C (1965–66).
7. E. S. Gaddis and W. B. Hall, The equilibrium of a bubble nucleus at a solid surface, paper 16, Thermodynamics and Fluid Mechanics Convention, Proc. Instn mech. Engrs. 182, Pt 3H (1967–68).
8. V. G. Jenson, Viscous flow around a sphere at low Reynolds number, *Proc. R. Soc.* **249A**, 346–366 (1959).
9. S. Goldstein, *Modern Developments of Fluid Dynamics*. Dover Publications (1965).
10. E. S. Gaddis, The thermal equilibrium of a vapour bubble on a heated solid surface, Ph.D. Thesis, University of Manchester (1968).

EFFETS DU MOUVEMENT LIQUIDE INDUIT PAR LE CHANGEMENT DE PHASE ET LA THERMOCAPILLARITE SUR L'EQUILIBRE THERMIQUE D'UNE BULLE DE VAPEUR

Résumé—On réalise l'étude théorique du mouvement d'un liquide induit autour d'une bulle de vapeur sur la surface d'un solide chauffé, par les effets de l'évaporation et de la condensation à la surface de la bulle et de la thermocapillarité. Ces résultats sont utilisés pour l'examen de l'équilibre thermique de la bulle de vapeur.

On trouve que, tandis que les effets de la convection induite par l'évaporation et la condensation sont petits, les effets de la thermocapillarité peuvent être importants dans la détermination de la température d'équilibre de la bulle.

DER EINFLUSS DER DURCH DEN PHASENÜBERGANG UND DIE THERMOKAPILLARITÄT HERVORGERUFENEN FLÜSSIGKEITSBEWEGUNG AUF DAS THERMISCHE GLEICHGEWICHT EINER DAMPFBLASE

Zusammenfassung—Es wurde eine theoretische Abschätzung der Flüssigkeitsbewegung gemacht, die in der Umgebung einer Dampfblase an einer beheizten festen Oberfläche durch Verdampfung und Kondensation an der Blasenoberfläche und durch Einflüsse der Thermokapillarität hervorgerufen wird. Die Ergebnisse wurden zur Prüfung des thermischen Gleichgewichts einer Dampfblase verwendet.

Es zeigte sich, dass die Einflüsse der durch Verdampfen und Kondensieren erzeugten Konvektion gering sind, die Einflüsse der Thermokapillarität dagegen möglicherweise bestimmend für die Blasentemperature im Gleichgewicht wirken.

ВЛИЯНИЕ ДВИЖЕНИЯ ЖИДКОСТИ В РЕЗУЛЬТАТЕ ФАЗОВЫХ ИЗМЕНЕНИЙ И ТЕРМОКАПИЛЛЯРНЫХ ПРОЦЕССОВ НА ТЕПЛОВОЕ РАВНОВЕСИЕ ПАРОВОГО ПУЗЫРЯ

Аннотация—Получена теоретическая оценка движения жидкости вблизи парового пузыря на нагретой твердой поверхности, Вызванного испарением и конденсацией на поверхности пузыря, а также термокапиллярными процессами. Результаты оценки использованы для исследования теплового равновесия пузыря.

Установлено, что влияние термокапиллярных процессов может быть существенным при определении температуры равновесного пузыря, тогда как влияние конвекции в результате испарения и конденсации незначительно.